Discrete breathers in classical ferromagnetic lattices with easy-plane anisotropy

Khalack, J. M.; Zolotaryuk, Yaroslav; Christiansen, Peter Leth

Published in:
Chaos

Link to article, DOI:
10.1063/1.1573611

Publication date:
2003

Document Version
Publisher's PDF, also known as Version of record

Discrete breathers in classical ferromagnetic lattices with easy-plane anisotropy

J. M. Khalack
Bogolyubov Institute for Theoretical Physics, National Academy of Sciences of Ukraine, Kyiv 03143, Ukraine;
Section of Mathematical Physics, IMM, Technical University of Denmark, DK-2800 Kgs. Lyngby, Denmark;
and Division of Physical Chemistry, Arrhenius Laboratory, Stockholm University, S-106 91 Stockholm, Sweden

Y. Zolotaryuk
Bogolyubov Institute for Theoretical Physics, National Academy of Sciences of Ukraine, Kyiv 03143, Ukraine
and Section of Mathematical Physics, IMM, Technical University of Denmark, DK-2800 Kgs. Lyngby, Denmark

P. L. Christiansen
Section of Mathematical Physics, IMM, Technical University of Denmark, DK-2800 Kgs. Lyngby, Denmark

(Received 23 October 2002; accepted 21 March 2003; published 22 May 2003)

Discrete breathers (nonlinear localized modes) have been shown to exist in various nonlinear Hamiltonian lattice systems. This paper is devoted to the investigation of a classical d-dimensional ferromagnetic lattice with easy plane anisotropy. Its dynamics is described via the Heisenberg model. Discrete breathers exist in such a model and represent excitations with locally tilted magnetization. They possess energy thresholds and have no analogs in the continuum limit. We are going to review the previous results on such solutions and also to report new results. Among the new results we show the existence of a big variety of these breather solutions, depending on the respective orientation of the tilted spins. Floquet stability analysis has been used to classify the stable solutions depending on their spatial structure, their frequency, and other system parameters, such as exchange interaction and local (single-ion) anisotropy. © *2003 American Institute of Physics.* [DOI: 10.1063/1.1573611]

The problem of energy *localization* in spatially distributed systems in condensed matter and biology is an important topic of modern physics. A lot of attention in the last several decades has been devoted to the phenomenon of localization due to spatial disorder. In particular, it is a well-known fact that lattice vibrations can localize themselves on impurities (creating so-called impurity localized modes). In this paper we deal with the relatively new concept of *intrinsic* localized modes (discrete breathers). These objects are spatially localized time-periodic lattice vibrations and their existence in *translationally invariant* (homogeneous) lattices has been proven rigorously. This remarkable phenomenon occurs in *nonlinear* lattices (lattices, governed by nonlinear equations of motion) and is based on the fact that the spectrum of the linear waves of the system under investigation is bounded and all possible resonances with the linear spectrum can be avoided. In this paper we are going to report on discrete breathers in classical ferromagnetic lattices with the easy-plane anisotropy. We are going to focus on the new type of solutions which have no continuum (soliton) analogs. Discrete breathers here have interesting spatial structure, consisting of a core of several spins, precessing around the hard axis and of tails, consisting of spins precessing with small amplitudes in the easy plane. These solutions possess energy thresholds so that their energy is separated from the energy of the ferromagnetic ground state by a gap. We also study linear stability of these excitations and how it depends on the spatial structure of the breather.

I. INTRODUCTION

The phenomenon of dynamical localization has been a subject of intense theoretical research. It is well known that classical Hamiltonian lattices possess periodic in time and localized in space solutions called discrete breathers (DB) or intrinsic localized modes (ILM). These are time-periodic and spatially localized coherent structures. A recent explosion of interest to discrete breathers has occurred due to the fact that they may exist in lattice models of interacting *identical* particles. Breathers in integrable continuum models (like, for example, the well known sine-Gordon equation) exist only due to high symmetry of the system, and are solitons. It has been proven rigorously[1] that in continuum nonintegrable systems like ϕ^4 breathers do not exist because their higher harmonics resonate with the linear spectrum. Discrete breathers are generic solutions of nonlinear lattice equations due to the fact that in discrete systems the linear spectrum is bounded from above and all possible resonances with the respective small-amplitude waves can be avoided.[2,3] A rigorous existence proof for discrete breathers has been given by MacKay and Aubry.[4] Several cases of experimental observation of discrete breathers have been reported (in Josephson junction

arrays,[5] arrays of weakly coupled waveguides,[6] low-dimensional crystals,[7] proteins,[8] and proteinlike crystals[9]).

Magnetic systems are ubiquitous in condensed matter. Due to spatial periodicity, the lattices of interacting spins are ideal candidates to observe discrete breathers. Here, we will concentrate on large spins, which may be described classically. Nonlinear waves in magnetic systems have extensively been studied during the last three decades.[10] The results of these studies provide a lot of information about the properties of solitary waves (particularly, breathers) in magnets, since it is possible in many cases to obtain explicit solutions to them. However, neglecting discreteness effects may lead to losing important features of nonlinear wave dynamics.

For instance, since only high symmetry continuous systems possess breather solutions, the area of potentially interesting models is artificially reduced. Another drawback of continuous systems is that the consideration of nontopological localized excitations is typically restricted to one-dimensional space.

An additional motivation for studying essentially discrete localized objects comes from the existence of materials with the exchange interaction of the order, or even much weaker than the single-ion anisotropy. As an example, these are quasi-one-dimensional magnets $[(CH_3)_3NH]NiCl_3 \cdot 2H_2O$ and $(C_9H_7NH)NiCl_3 \cdot 1.5H_2O$ (Ref. 11) or layered antiferromagnets $(CH_2)_n(NH_3)_2MnCl_4$, $(C_nH_{2n+1}NH_3)_2MnCl_7$.[12]

In the last decade, a number of papers has appeared, where localized modes in magnets were treated as essentially discrete objects[13–16] (also, the attempt of experimental observation of discrete breathers in antiferromagnets has been made recently[17]).

A new approach, based on the concept of the *anticontinuum limit*, has been applied to spin systems. It was used to prove breather existence rigorously for easy-axis ferromagnets.[18,19] Also, Zolotaryuk and co-workers[18] have used this approach to find numerically a new type of breather solution in easy-plane ferromagnets which have no continuum analog. These solutions consist of a core of spins precessing around the hard (single-ion anisotropy) axis and tails of spins precessing in the easy plane. The aim of this work is to present breather excitations for spin lattices, for which the symmetries will not allow for a similar mode construction in spatially continuous cases. We review the previous results[18] on existence and properties of these breathers and also show new results on their linear stability.

This paper is organized as follows: The next section presents the model Hamiltonian and the equations of motion. In Sec. III, we review the main properties of discrete breather solutions. In Sec. IV, we study their linear stability. Section V presents discrete breathers on a two-dimensional spin lattice. Discussions and conclusions are given in Sec. VI.

II. THE MODEL

Consider a lattice of classical spins described by the Hamiltonian with isotropic Heisenberg exchange interaction and single-ion anisotropy,

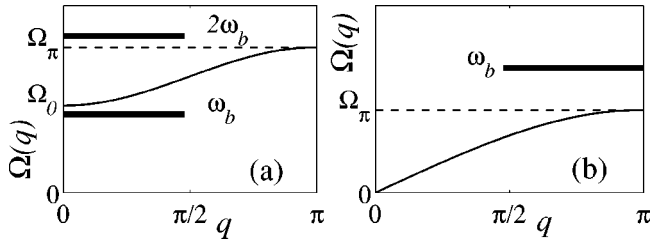

FIG. 1. Magnon dispersion laws for the easy-axis (a) and easy-plane (b) ferromagnetic chains.

$$H=-\frac{J}{2}\sum_{\mathbf{n}\neq\mathbf{n}'}\sum_{\alpha=(x,y,z)} S_{\mathbf{n}}^{\alpha}S_{\mathbf{n}'}^{\alpha}-D\sum_{\mathbf{n}} S_{\mathbf{n}}^{z2}. \tag{1}$$

Here $S_{\mathbf{n}}^{x},S_{\mathbf{n}}^{y},S_{\mathbf{n}}^{z}$ are the $\mathbf{n}$th spin components ($\mathbf{n}$ labels lattice sites) that satisfy the normalization condition,

$$S_{\mathbf{n}}^{x2}+S_{\mathbf{n}}^{y2}+S_{\mathbf{n}}^{z2}=S^2. \tag{2}$$

For simplicity, the total spin magnitude can be normalized to unity: $S=1$. The constant J is the exchange integral and D is the on-site anisotropy constant. We focus on the ferromagnetic case $J>0$ (if $J<0$ we would have an antiferromagnet). It is assumed here that spin $\mathbf{S_n}$ is rather large and the lattice can be treated classically.

The equations of motion for the spin components in the d-dimensional spin chain with nearest-neighbor interactions are the discrete version of the well known Landau–Lifshitz equations,

$$\dot{\mathbf{S}}_{\mathbf{n}}=[\mathbf{S_n}\times\mathbf{H_n^{eff}}],\quad \mathbf{H_n^{eff}}=-\nabla_{\mathbf{S_n}}H. \tag{3}$$

If $D>0$ the spin lattice has an easy-axis anisotropy with Z being an easy axis. This means that the ground state of the chain corresponds to the case when all spins are aligned along the easy axis. We are interested in the case of an easy-plane anisotropy, i.e., $D<0$. In this case the ground state of the lattice corresponds to spins lying in the easy plane, which is XY. Note that the ground state is degenerate, so that the spins can be oriented arbitrarily in the XY plane, but they must stay parallel to each other. Without loss of generality, the ground state of the one-dimensional lattice can be assumed to be

$$S_n^x=1,\quad S_n^y=S_n^z=0. \tag{4}$$

Linearizing the equations of motion in the vicinity of this ground state, we obtain the following dispersion law:

$$\Omega^2(q)=J^2(1-\cos q)^2+2J|D|(1-\cos q),$$
$$\Omega_0^2=\Omega^2(0)=0,\quad \Omega_\pi^2=\Omega^2(\pi)=4J(J+|D|). \tag{5}$$

In Fig. 1 the dispersion laws for the easy-axis [panel (a)] and easy-plane [panel (b)] ferromagnets are shown. The spectrum of the easy-axis system has a gap while the easy-plane case is gapless, similarly to phonon spectrum of ''acoustic'' lattices (Fermi–Pasta–Ulam, for example).

A necessary condition for the existence of discrete breathers is nonresonance of the breather frequency ω_b or any of its multiples with the magnon band,

$$n\omega_b\neq\Omega(q),\quad n=0,1,2,\ldots\ . \tag{6}$$

In the easy-axis case the breather frequency lies in the gap, so one must make sure that higher multiples of breather frequency, i.e., $2\omega_b, 3\omega_b, \ldots$, will not appear in the magnon spectrum [see Fig. 1(a)]. There is no gap in the easy-plane spectrum, therefore the breather frequencies should lie above its upper edge [see Fig. 1(b)].

One must note that in the previously studied easy-axis cases (both ferro- and antiferromagnetic) breathers can be viewed as localized spin excitations with the spins precessing around the easy axis, so that the effective radius of this precession decreases to zero as $n \to \pm\infty$. Since exchange is isotropic, the S^z-component is conserved in the solution, and therefore the separation of the time and the space variables of the form,

$$S_n^{\pm} = S_n^x \pm i S_n^y = A_n e^{\pm i\omega_b t} \tag{7}$$

is possible in the Landau–Lifshitz equations. Thus, a breather in this case has only one harmonic and can be called *monochromatic*. A similar situation occurs in the easy-plane ferromagnet under the strong magnetic field directed parallel to the Z axis, studied by Wallis and co-workers.[14] Strong magnetic field in this case turns the system effectively into an easy-axis one. In the monochromatic case there is only one resonance to be avoided, namely, the resonance of the main breather frequency with the magnon band, i.e., $\omega_b \neq \Omega(q)$. This is not the case when the symmetry of the system in XY is broken, for example, by exchange anisotropy[18] or by biaxial single-ion anisotropy.[15] The case we are going to consider below will also include nonmonochromatic breathers.

III. PROPERTIES OF BREATHER SOLUTIONS

In this section we give a review of the properties of the discrete breather solutions, obtained by Zolotaryuk and co-workers.[18] Following MacKay and Aubry,[4] the concept of the anticontinuum (AC) limit has been applied[18] to discrete breathers in the easy-plane ferromagnetic lattices. The main idea of the AC limit consists in decoupling the lattice sites and exciting only one or a small number of them, n_r, keeping all the other sites in the ground state. Then, upon switching on the interaction, the persistence of the localized solution is shown. As a prerequisite for the successful existence proof and continuation of the breather solution, the initial ''decoupled'' periodic orbit must be anharmonic and the breather frequency and all its multiples should not resonate with the magnon band. The implementation of the AC limit can be achieved by setting $J=0$ and exciting one or several spins, so that they should start to precess around the hard axis with the frequency ω_b. Solving discrete Landau–Lifshitz equations (3) in the AC limit yield the precessing frequency $\omega_b = 2|D|S_0$ with S_0 being the z-projection of the precessing spin. If the nonresonance condition $\omega_b \neq \Omega_\pi = 0$ is satisfied, the breather solution can be continued.

For nonzero J, initially nonexcited spins start to precess with small amplitudes around the X-axis, while the plane of precession of the ''out-of-plane'' spin is no longer parallel to the easy plane, being slightly tilted (as shown schematically in Fig. 2).

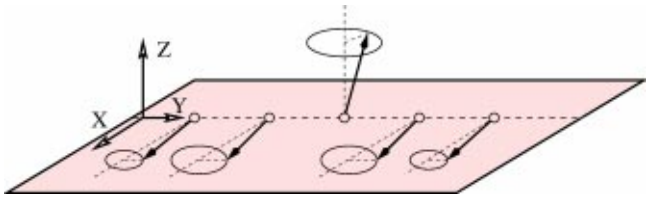

FIG. 2. Schematic representation of the discrete breather with one ''out-of-plane'' spin in the easy-plane ferromagnet.

It is possible to create different breather configurations depending on respective orientation of the ''excited'' (out-of-plane) spins. We will classify the possible breather solutions depending on their anticontinuum (AC) configuration with the help of the following coding sequences. A precessing spin turned upwards ($S_n^z > 0$) will be represented by $\uparrow$, the spin directed downwards ($S_n^z < 0$) will be represented by $\downarrow$. Zeros correspond to spins in the ground state. Respective orientation of spins in the X direction can also be incorporated in the coding sequence: $+$ will stand for $S_n^x > 0$ and $-$ will stand for $S_n^x < 0$. With one ''out-of-plane'' precessing spin ($n_r = 1$), there are two equivalent breather configurations, $(\cdots 000\uparrow 000\cdots)$ and $(\cdots 000\downarrow 000\cdots)$. Now we discuss the possible breather configurations with two precessing ''out-of-plane'' spins ($n_r = 2$) with numbers n_0 and n_0+1. A breather configuration with two parallel spins directed upwards $\mathbf{S_{n_0} = S_{n_0+1}}$, will be represented by the coding sequence $(\cdots 000\uparrow\uparrow 000\cdots)$. If there is a phase shift π between precession of these spins, so that $S_{n_0}^x = -S_{n_0+1}^x$ and $S_{n_0}^y = -S_{n_0+1}^y$, this configuration will be denoted as $(\cdots 000\uparrow^+\uparrow^- 000\cdots)$. Reflections of the above configuration with respect to breather center or with respect to the easy plane do not change it, thus, configurations $(\cdots 000\uparrow^-\uparrow^+ 000\cdots)$, $(\cdots 000\downarrow^-\downarrow^+ 000\cdots)$, and $(\cdots 000\downarrow^+\downarrow^- 000\cdots)$ are equivalent to the original one. If spins are antiparallel ($S_{n_0}^z > 0, S_{n_0+1}^z < 0$) there are two possible nontrivial configurations: $S_{n_0}^x = -S_{n_0+1}^x$, $S_{n_0}^y = S_{n_0+1}^y$ configuration will be represented as $(\cdots 000\uparrow^+\downarrow^- 000\cdots)$ and $S_{n_0}^x = S_{n_0+1}^x$ and $S_{n_0}^y = -S_{n_0+1}^y$ will be denoted as $(\cdots 000\uparrow\downarrow 000\cdots)$. This coding sequence can be easily generalized on the arbitrary number of the out-of-plane spins. For example, a breather with six out-of-plane spins at sites $n_0, n_0+1, \ldots, n_0+5$ with first three spins having $S_n^z > 0$ and last three $S_n^z < 0$ and, also, $S_{n_0}^x = S_{n_0+1}^x = S_{n_0+2}^x$, $S_{n_0+3}^x = -S_{n_0+2}^x$, $S_{n_0+3}^x = S_{n_0+4}^x = S_{n_0+5}^x$ will be denoted as $(\cdots 000\uparrow^+\uparrow^+\uparrow^+\downarrow^-\downarrow^-\downarrow^- 000\cdots)$.

A. Computation of breathers

For numerical simulations it is convenient to use stereographic coordinates. The new coordinates incorporate the normalization condition and reduce the problem with three unknown real functions S_n^x, S_n^y, and S_n^z per site to the problem with one unknown complex function ξ_n per site,

$$\xi_n = \frac{S_n^x + iS_n^y}{1 + S_n^z}. \tag{8}$$

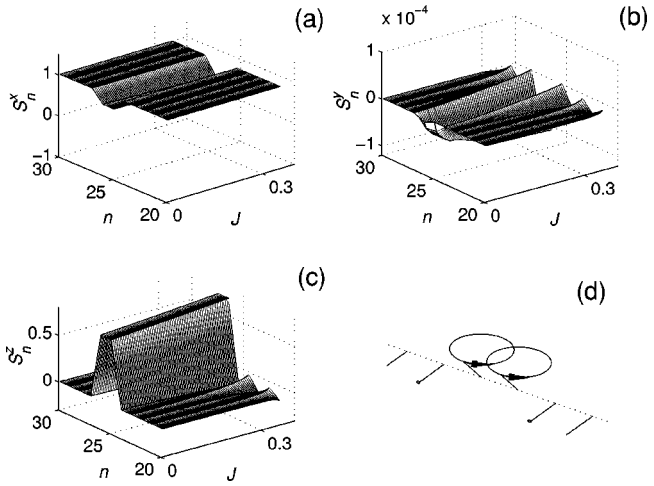

FIG. 3. Profiles of the spin components of the (↑↑) breather as a function of the exchange J [panels (a), (b), and (c)]. Panel (d) shows the breather profile at $J=0.1$. Other parameters are $D=-1$, $\omega=1.4$.

The inverse transform is given by

$$S_n^x=\frac{\xi_n+\xi_n^*}{1+|\xi_n|^2},\quad S_n^y=\frac{1}{i}\,\frac{\xi_n-\xi_n^*}{1+|\xi_n|^2},\quad S_n^z=\frac{1-|\xi_n|^2}{1+|\xi_n|^2}. \tag{9}$$

In these new coordinates the discrete Landau–Lifshitz equations take the form,

$$i\dot{\xi}_n=\frac{J}{2}\left[\frac{\xi_{n-1}-\xi_n^2\xi_{n-1}^*}{1+|\xi_{n-1}|^2}+\frac{\xi_{n+1}-\xi_n^2\xi_{n+1}^*}{1+|\xi_{n+1}|^2}-\xi_n\left(\frac{1-|\xi_{n-1}|^2}{1+|\xi_{n-1}|^2}+\frac{1-|\xi_{n+1}|^2}{1+|\xi_{n+1}|^2}\right)\right]-2D\xi_n\frac{1-|\xi_n|^2}{1+|\xi_n|^2}. \tag{10}$$

The computation of the discrete breathers is done, using the Newton method.[2] Discrete breather periodic orbits are zeroes of the Newton map,

$$\mathbf{F}=\mathbf{u}-\hat{I}_T\mathbf{u},\quad \mathbf{u}=\{\mathrm{Re}\,\xi_n,\mathrm{Im}\,\xi_n\}. \tag{11}$$

Here the operator $\hat{I}_T$ stands for integration of the Landau–Lifshitz equations (10) with initial conditions $\mathbf{u}=\{\mathrm{Re}\,\xi_n,\mathrm{Im}\,\xi_n\}$ over the breather period $T=2\pi/\omega_b$. As an example, in Fig. 3 we show the profiles of the (↑↑) (Ref. 20) breather as a function of the exchange integral J. They have been computed in the chain of $N=30$ spins starting from the AC limit. Panels (a), (b), and (c) show the snapshots of the S^x, S^y, and S^z components of the spin, respectively. Panel (d) shows the structure of the breather for $J=0.1$. We describe the dynamics of the spins during one breather period with circles.

B. Breather behavior as a function of frequency and system parameters

Depending on its frequency, the breather width changes. When the frequency approaches the upper edge of the linear band from above, the breather becomes more delocalized. However, this does not qualitatively influence its core structure, i.e., the effective precession axis of the central spin is not continuously tilted toward the X-axis upon lowering the breather frequency down to the linear band edge. The central spin(s) dynamics can be viewed as a periodic (closed) orbit of a point confined to the unit sphere. Let the XY plane be the equatorial one. Then, for high breather frequencies, the point performs small circles around the north (or south) pole. Lowering the breather frequency does not change the fact that the loop still encircles the Z-axis. Thus, the breather solution cannot be deformed into a slightly perturbed and weakly localized magnon, and, thus, the easy-plane ferromagnet lattice supports the breather solutions with a local magnetization tilt that have no continuum analogs. This gives us a reason to believe that there exists an energy threshold (gap) which separates the energy of the discrete breather from the ground state.[18] This fact can be easily understood: since there is a finite number of spins precessing around the hard axis no matter what the breather frequency, their energy is always nonzero.

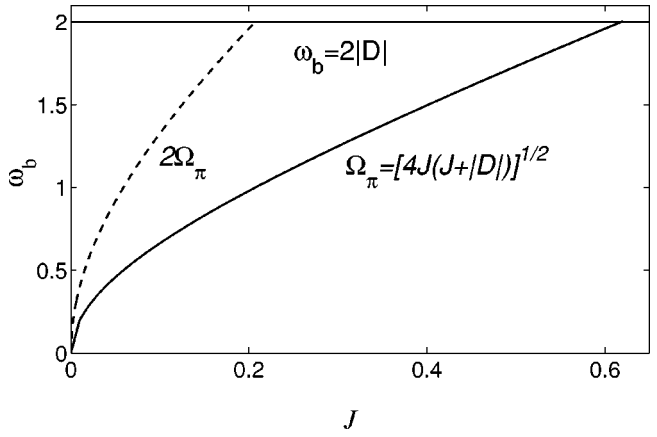

FIG. 4. Breather existence diagram for $D=-1$. The dashed line shows the border of parametric resonance, $\omega_b/2=\Omega_\pi$.

Energy thresholds have been estimated analytically[18] in the limit of small exchange J. Ignoring the displacements of all in-plane spins, the threshold energy (normalized to the ground state energy) for the breather with n_r out-of-plane precessing spins has been obtained:

$$E\approx 2n_r|D|S_0^{z2}. \tag{12}$$

Here $S_0^z=\omega_b/2|D|$ is the Z-component of the precessing spin in the AC limit. The factor 2 stems from the fact that we should take into account the contribution of the breather tails.

Increase of the frequency leads to decrease of the precession radius of the central spin. In the AC limit, the upper bound for the breather frequency is determined by $\omega_b=2D$ that corresponds to the central (precessing) spin being parallel to the Z-axis. This bound continues to exist when the exchange is switched on. After reaching this frequency threshold, the breather becomes a stationary (time-independent) solution. The existence of such a solution has been verified numerically by solving the time-independent Landau–Lifshitz equations.

Thus, in the frequency domain breather solutions are limited from below by the upper edge of the magnon band and from above by the value $\omega_b\simeq 2|D|$. In Fig. 4 we show

the breather existence diagram in the plane (J,ω_b) with $D=-1$. Breather solutions exist in the segment encircled by the lines $\omega_b=2|D|$ and $\omega_b=\Omega_\pi=\sqrt{4J(J+|D|)}$. Maximal value of exchange J for which breathers exist can be easily determined for each frequency from the above equation. Thus, $J_{\max}(\omega_b,D)=[\sqrt{D^2+\omega_b^2}-|D|]/2$. For the highest possible frequency, $\omega_b=2|D|$, $J_{\max}(2|D|,D)=(\sqrt{5}-1)|D|/2$. The border of the parametric resonance $(\omega_b/2=\Omega_\pi)$ equals $J_{\text{param}}=[\sqrt{4D^2+\omega_b^2}-2|D|]/4$, so breathers are expected to be stable within the interval $0<J<J_{\text{param}}$. However, in order to check the implication of different resonances one should investigate breather stability in a more systematic way.

IV. STABILITY OF BREATHER SOLUTIONS AND THEIR ASYMPTOTIC PROPERTIES

The linear stability analysis of the discrete breathers is based on Floquet theory (more details can be found in the review by Aubry[3]). Suppose $\{\xi_n^{(0)}(t)\}$ is the breather periodic orbit for a lattice of N spins. Then we linearize Eq. (10) around it: $\xi_n(t)=\xi_n^{(0)}(t)+\varepsilon_n(t)$ and find the Floquet (monodromy) matrix $\hat{\mathcal{M}}$, which satisfies the following equation:

$$\begin{bmatrix}\text{Re}\,\varepsilon_n(T)\\ \text{Im}\,\varepsilon_n(T)\end{bmatrix}=\hat{\mathcal{M}}\begin{bmatrix}\text{Re}\,\varepsilon_n(0)\\ \text{Im}\,\varepsilon_n(0)\end{bmatrix}. \tag{13}$$

There are $2N$ eigenvalues λ_n of this matrix. If all of them are found to be located on the unit circle of the complex plane, then according to the Floquet theorem, the periodic orbit is stable, otherwise it is unstable. If one looks at the corresponding eigenvectors of the Floquet matrix, there are both spatially delocalized vectors, corresponding to the linear magnon spectrum and spatially localized vectors, whose origin is localized nature of the breather itself.

The simulations have been performed with different boundary conditions: free ends, fixed ends $[\mathbf{S_1}=(1,0,0),\ \mathbf{S_N}=(1,0,0)]$ and one end of the chain fixed $[\mathbf{S_1}=(1,0,0)]$ and the other one is free. No principal differences have been observed since the size of the chain is considerably larger then the breather characteristic size. All the results reported below are for the fixed ends unless stated otherwise.

A. Breather stability as a function of exchange

Consider first the stability properties of the breather solutions at the fixed frequency $\omega=1.4$. In Fig. 5 we show how the eigenvalues of the one spin $(\uparrow)$ breather periodic orbit change while the exchange interaction J is increased. We see that it is stable in the small segment in the vicinity of $J=0$ and later on an instability develops. The structure of the Floquet spectrum is the following: there is a band of delocalized modes associated with the magnon spectrum, and the internal mode which lies between the lowest delocalized mode and the phase shift mode at $+1$.

Upon increasing the exchange J this internal mode moves down and collides with itself on the real axis at $+1$ [see insets of Fig. 5(a)]. This happens at rather small exchanges ($J=0.054$, as for the case of $N=50$ shown in Fig. 5). Once lost, stability is never recovered. The shape of the internal mode is shown in Figs. 5(c)–5(e). The main direction of instability is in the S^y component, and it favors formation of a torsional displacement on the breather in XY plane. In order to understand better the nature of the instability of the $(\uparrow)$ breather, we have investigated more closely the behavior of its Floquet eigenvalues in the neighborhood of $J=0$. The internal mode lies under the lowest delocalized mode. However, the Floquet spectrum is discrete due to the fact that N is finite. As N increases, the spectrum becomes more and more dense and, eventually, becomes continuous as $N\to\infty$. Thus, the internal mode is squeezed in between the lowest delocalized mode and real axis $(\text{Arg}\,\lambda=0)$. Thus, collision of the eigenvalue associated with the internal mode at $+1$ will take place closer and closer to $J=0$ as long as N is increased, as shown in Fig. 6. Therefore we can conclude that for realistic systems where N is large, $(\uparrow)$ breathers are unstable.

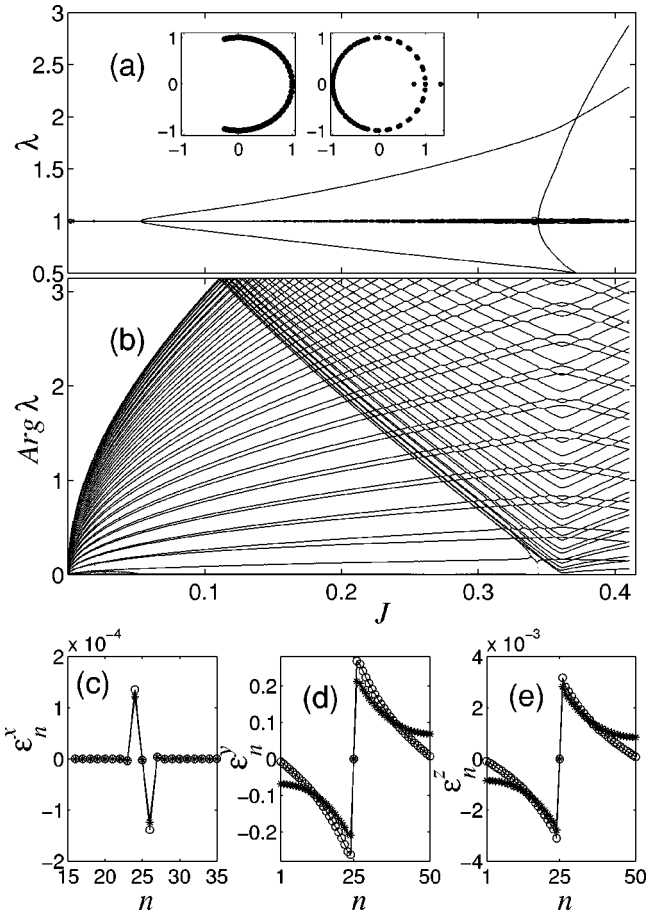

FIG. 5. Eigenvalues (a), (b) and eigenvectors (c)–(e) of the breather periodic orbit $(\uparrow)$ as a function of J at a frequency of $\omega_b=1.4$ and for $N=50$. Panels (a) and (b) correspond to the absolute value and its argument, respectively. The left and right insets in panel (a) show the positions of the Floquet eigenvalues on the unit circle for $J=0.04$ and $J=0.2$, respectively. Panels (c), (d), and (e) show the x, y, and z components of the unstable eigenvector at $J=0.1$ for free (+) and fixed (○) boundaries.

Now we turn our attention to the case of two out-of-plane spins. Four different breather configurations are possible: $(\uparrow\uparrow)$, $(\uparrow^+\uparrow^-)$, $(\uparrow\downarrow)$, and $(\uparrow^+\downarrow^-)$. We start with the simplest configuration, $(\uparrow\uparrow)$. The stability picture is shown of Fig. 7. Careful inspection of the evolution of the Floquet eigenvalues with J first reveals very weak instabilities which start to develop at $J_{\text{param}}=[\sqrt{4D^2+\omega_b^2}-2|D|]/4=(\sqrt{5.96}$

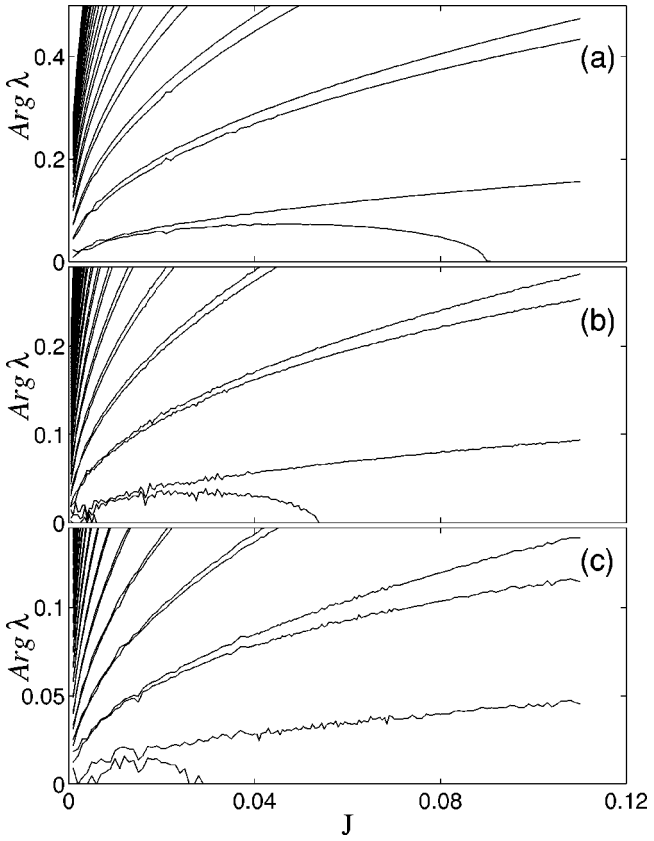

FIG. 6. Zoomed Fig. 5(b) for $N=30$ (a), 50 (b), and 100 (c). Ripples appear due to computational error.

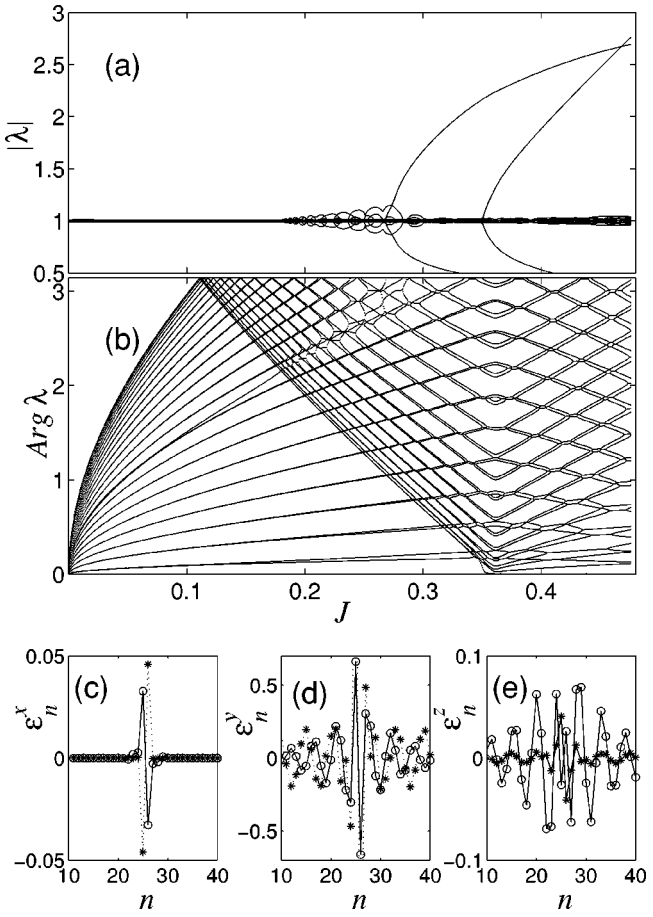

FIG. 7. The same as Fig. 5 for the $(\uparrow\uparrow)$ breather. The eigenvectors of the unstable mode (see text for details) are given for $J=0.17$ $(*)$ and $J=0.28$ $(\bigcirc)$.

$-2)/4\simeq 0.11$. These instabilities are caused by the delocalized eigenvalues colliding with their complex-conjugate counterparts at -1 on the unit circle. Therefore they can be referred to as ''parametric'' instabilities (caused by the parametric resonance).

It has been shown[21] that these instabilities decay as the size of the lattice increases and disappear as $N\to\infty$. Even for $N=50$ they are too small to be seen in Fig. 7(a). Thus, the parametric instabilities are of limited interest. The more prominent Hopf-type instability starts to grow at $J=0.181$ [the ''bubbles'' in Fig. 7(a)] due to a collision of an internal mode with the leading edge of the magnon band. The internal mode can be easily spotted in Fig. 7(b) since it is not parallel to the lines corresponding to the delocalized mode. This mode is not completely localized since it lies in the magnon spectrum. It is rather ''quasilocalized,'' as one can see from Figs. 7(c)–7(e). Collision of this mode with its counterpart at -1 on the unit circle at $J\approx 0.27$ triggers the instability which does not recover any longer while J is increased. The unstable eigenvectors are antisymmetric and the direction in which the instability is most pronounced is the S^y direction. The eigenvector is antisymmetric with respect to the breather center. As the exchange J increases the precessing spins interact stronger and stronger with their neighboring ''in-plane'' spins. The shape of the eigenvector shows that ''in-plane'' spins pull the ''out-of-plane'' precessing spins so that the latter can eventually fall into the easy plane destroying the breather.

Now we turn our attention to the next breather type, namely $(\uparrow^+\uparrow^-)$. Here both ''out-of-plane'' spins are parallel but precess with a phase difference π so that their S^x components have opposite values. In Fig. 8 we show how the Floquet eigenvalues develop as exchange J is increased. This configuration is unstable for all values of J due to the unstable internal mode whose eigenvalue lies on the positive part of the real axis of the unit circle [see the inset of Fig. 8(a)]. The asymmetric shape of the mode [see panels (c)–(e) of Fig. 8] suggests the instability wants to ''correct'' the existing phase lag between precession of the two out-of-plane spins. This is understood from the general physical argument—if the exchange is ferromagnetic, thus parallel alignment of spins is the most favorable one energetically.

The next configuration, $(\uparrow\downarrow)$ also develops an instability starting from the AC limit as it can be seen in Fig. 9. The instability is caused by the internal mode, which, similarly to the case $(\uparrow^+\uparrow^-)$, also has an eigenvalue moving from $+1$ along the real axis of the unit circle. The shape of the unstable internal mode (eigenvector) is shown in panels (c)–(e) of Fig. 9. It suggests that the instability has a nature, similar to the $(\uparrow^+\uparrow^-)$ case. The ferromagnetic interaction tends to align spins in the energetically most favorable position.

Finally we consider the last configuration, $(\uparrow^+\downarrow^-)$, which in some sense can be considered as a ''combination''

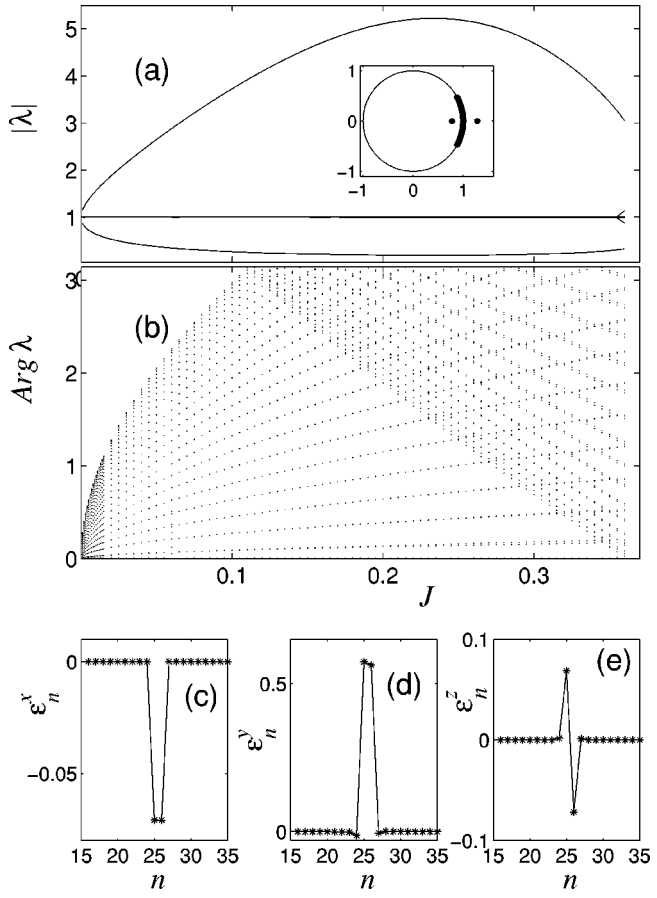

FIG. 8. The same as Fig. 5 for the $(\uparrow^+\uparrow^-)$ breather. The eigenvalues in the inset and the eigenvectors are shown for $J=0.03$.

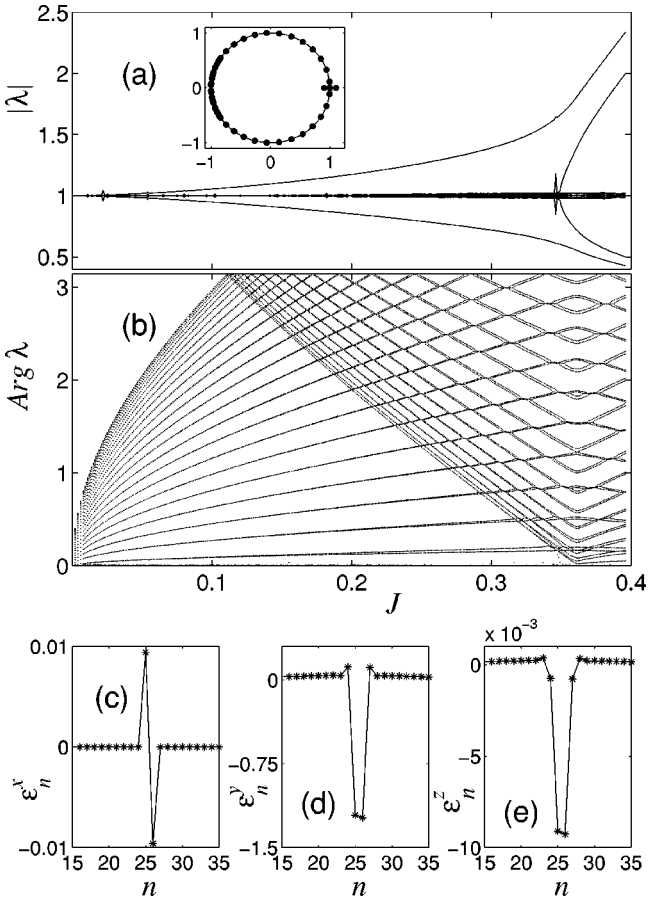

FIG. 9. The same as Fig. 5 for the $(\uparrow\downarrow)$ breather. The eigenvalues in the inset are for $J=0.15$ and the eigenvectors are shown for $J=0.1$.

of the previous two, $(\uparrow^+\uparrow^-)$ and $(\uparrow\downarrow)$. However, as shown in Fig. 10, this configuration appears to be stable. As the exchange J is increased, parametric instabilities start to appear, however, as we have mentioned before, they will not affect significantly breather dynamics as $N\to\infty$.

For the breathers with three out-of-plane spins it has been found that the configuration $(\uparrow\uparrow\uparrow)$ is stable starting from the AC limit up to some critical value of J. The Floquet spectrum of this periodic orbit possesses two internal modes [note there was only one such a mode in the $(\uparrow\uparrow)$ configuration] which are positioned in between the delocalized modes. The instability is triggered when the respective eigenvalues collide at -1 on the unit circle. The other stable configuration is $(\uparrow^+\uparrow^+\downarrow^-)$. Further investigation of the breather stability has shown that addition of a parallel spin to the stable breather does not destroy its stability. In other words, since $(\uparrow\uparrow)$ is stable, $(\uparrow\uparrow\uparrow)$ is also stable as well as any configuration of this type $(\uparrow\cdots\uparrow\uparrow)$ with an arbitrary number of parallel out-of-plane spins. Similarly, since $(\uparrow^+\downarrow^-)$ is stable, we have checked that $(\uparrow^+\uparrow^+\downarrow^-)$, $(\uparrow^+\uparrow^+\uparrow^+\downarrow^-)$, $(\uparrow^+\uparrow^+\downarrow^-\downarrow^-)$, $(\uparrow^+\uparrow^+\uparrow^+\uparrow^+\downarrow^-)$, $(\uparrow^+\uparrow^+\uparrow^+\downarrow^-\downarrow^-)$, and any configuration which can be obtained by adding a parallel spin to the edge of the cluster, are stable.

Another class of stable solutions for higher number of out-of-plane spins contains the configurations that consist of clusters of parallel spins [for example, $(\uparrow\uparrow\uparrow)$ or $(\downarrow\downarrow)$]: $(\uparrow\uparrow\downarrow\downarrow)$, $(\uparrow\uparrow\uparrow\downarrow\downarrow)$, $(\uparrow\uparrow\uparrow\downarrow\downarrow\downarrow)$. Thus, any superpositions of stable con-

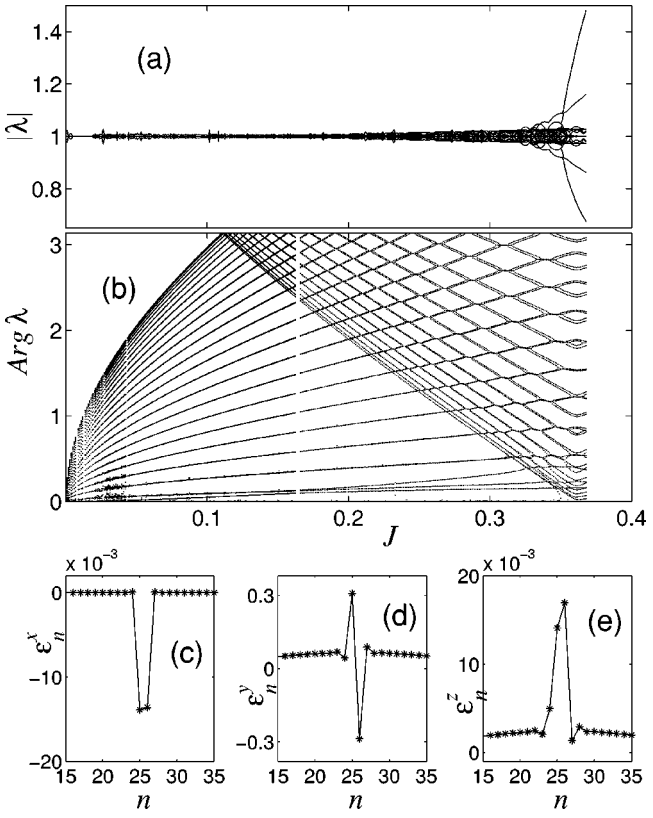

FIG. 10. The same as Fig. 5 for the $(\uparrow^+\downarrow^-)$ breather. Panels (c)–(e) show the lowest lying eigenvector for $J=0.1$.

TABLE I. List of stable breather configurations. Because there are too many possible breather configurations for $n_r>3$ we have plotted only several of the stable ones. See text for details.

n_r	Stable configurations
1	...
2	$(\uparrow\uparrow)$, $(\uparrow^+\downarrow^-)$
3	$(\uparrow\uparrow\uparrow)$, $(\uparrow^+\uparrow^+\downarrow^-)$
4	Not complete; $(\uparrow\uparrow\uparrow\uparrow)$, $(\uparrow\uparrow\downarrow\downarrow)$, $(\uparrow^+\uparrow^+\uparrow^+\downarrow^-)$, $(\uparrow^+\uparrow^+\downarrow^-\downarrow^-)$, $(\uparrow^+\downarrow^-\downarrow^-\uparrow^+)$, $(\uparrow^+\uparrow^+\downarrow^+\uparrow^-)$
5	Not complete; $(\uparrow\uparrow\uparrow\uparrow\uparrow)$, $(\uparrow\uparrow\uparrow\downarrow\downarrow)$, $(\uparrow^+\uparrow^+\uparrow^+\uparrow^+\downarrow^-)$, $(\uparrow^+\uparrow^+\uparrow^+\downarrow^-\downarrow^-)$
6	Not complete; $(\uparrow\uparrow\uparrow\uparrow\uparrow\uparrow)$, $(\uparrow\uparrow\uparrow\downarrow\downarrow\downarrow)$, $(\uparrow\uparrow\downarrow\downarrow\uparrow\uparrow)$, $(\uparrow^+\uparrow^+\uparrow^+\downarrow^-\downarrow^-\downarrow^-)$

figurations with parallel spins are stable for the case of the intercluster boundaries of the type $(\cdots\uparrow\downarrow\cdots)$. Note that breather configurations $(\uparrow\uparrow\downarrow)$ or $(\uparrow\uparrow\uparrow\downarrow)$ are unstable since a one-spin breather $(\uparrow)$ is unstable. To summarize, in Table I we show the possible stable configurations for a different number of ''out-of-plane'' spins. For $n_r=4,5,6$ we have not shown all possible stable configurations, since the number of possible breather configurations grows sharply as n_r increases.

In Fig. 11 we show the dependence of Floquet eigenvalues on the exchange J. It is interesting to note that while the ''bubbles'' associated with the Hopf-type instabilities due to collision of the internal mode with the linear delocalized modes appear at about the same J, the significant instabilities driven by the excursion of the internal modes along the real axis after collision with their counterparts at -1 appear at larger J as long as n_r is increased. The more out-of-plane spins present in the breather solution, the more internal modes it possesses. As a result, the excursion of one internal mode out of the unit circle becomes shorter, and the corresponding instability becomes less pronounced. Furthermore, the most significant instability is associated with the lowest lying internal mode, so this instability appears at a larger exchange for increased n_r. Another interesting feature associated with the breather symmetry is a somewhat different instability picture for even [Figs. 7(a), 11(b), 11(d)] and odd [Figs. 11(a), 11(c)] number of out-of-plane spins. The case of the even n_r is characterized with the higher respective instability than the case of the odd n_r.

Physically, the decrease of the instability for the breathers with large n_r can be explained by the fact that with the larger number of ''out-of-plane'' spins the energy gap that separates breathers from the magnons is larger and it is much harder for the exchange interaction to bring the precessing spins back into the easy plane.

B. Breather stability as a function of its frequency

It is interesting to investigate how breather stability depends on its frequency. It has been shown that breathers exist within the following frequency domain: $\Omega_\pi=\sqrt{4J(J+|D|)}<\omega_b<2|D|$. In Fig. 12 we show how breather stability for the configuration $(\uparrow\uparrow)$ changes as the exchange is increased starting from the AC limit. We have taken different values of breather frequency: $\omega_b=0.7,1.4,1.6,1.8,1.98$.

The figure clearly shows that the higher the frequency the more stable is the breather solution. This can be easily explained with the help of Fig. 4. Breather instabilities are

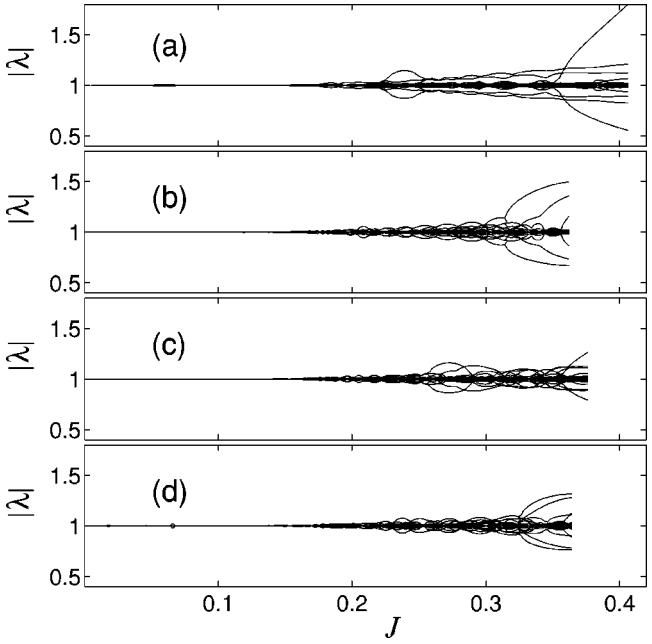

FIG. 11. Dependence of the absolute value of the Floquet eigenvalues on the exchange integral J for different breather configurations: $(\uparrow\uparrow\uparrow)$ (a), $(\uparrow\uparrow\uparrow\uparrow)$ (b), $(\uparrow\uparrow\uparrow\uparrow\uparrow)$ (c), $(\uparrow\uparrow\uparrow\uparrow\uparrow\uparrow)$ (d). The breather frequency is $\omega_b=1.4$.

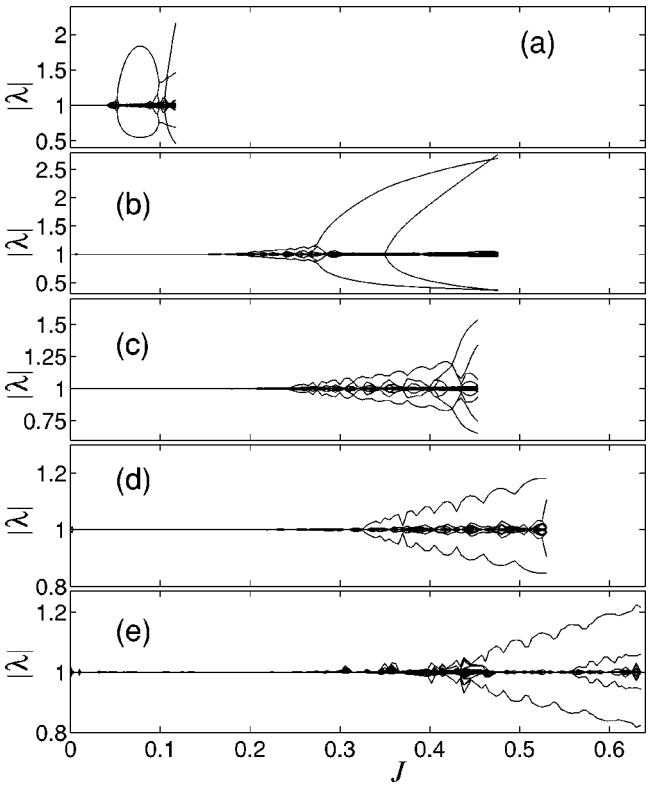

FIG. 12. Dependence of the absolute value of the Floquet eigenvalues of the $(\uparrow\uparrow)$ breather on exchange J for different frequencies: (a) $\omega_b=0.7$, (b) $\omega_b=1.4$, (c) $\omega_b=1.6$, (d) $\omega_b=1.8$, and (e) $\omega_b=1.98$.

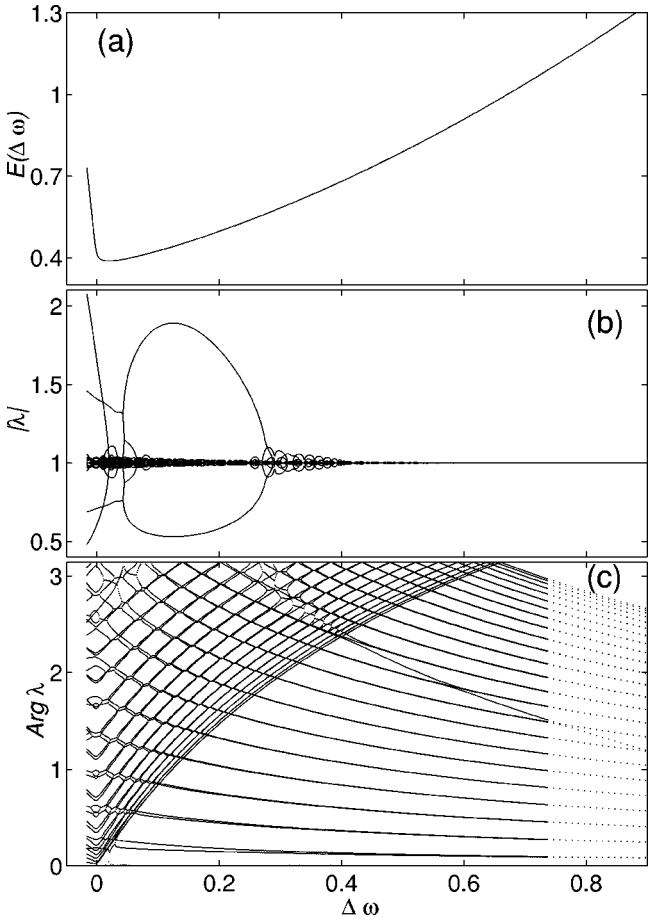

FIG. 13. Breather behavior as a function of detuning $\Delta\omega=\omega_b-\Omega_\pi$ for $J=0.1$: (a) dependence of the normalized breather energy $E=H-J(N-1)/2$; (b), (c) behavior of the Floquet eigenvalues.

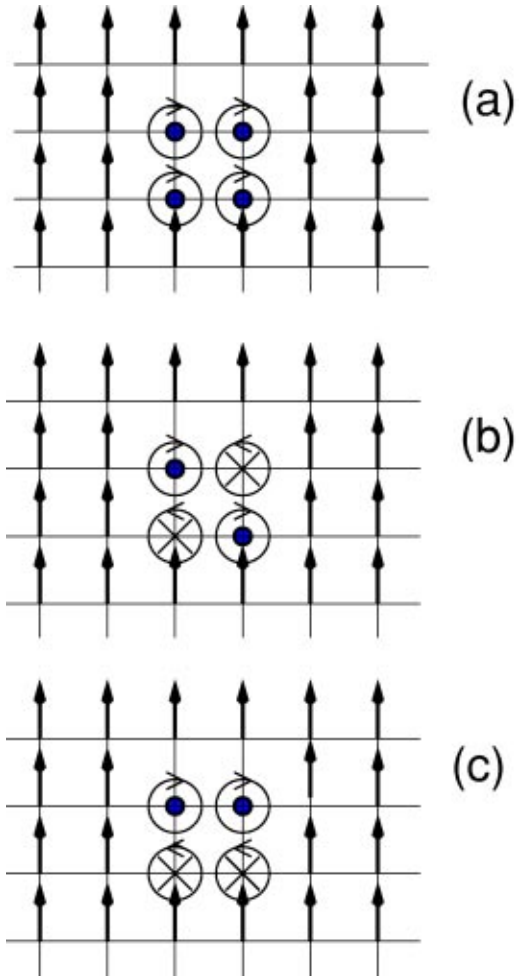

FIG. 14. Schematical representation of some possible configurations of discrete breathers with four precessing spins.

caused by parametric resonances (collisions of Floquet eigenvalues at -1) either of delocalized modes or of internal modes. Therefore, the parametric resonance takes place at larger J's if ω_b is increased.

We also investigate the breather behavior as its frequency is decreased, $\omega_b\to\Omega_\pi$. As it has been discussed in the previous section, when approaching to the upper bond of the magnon spectrum, the breather does not change into a weakly localized magnon but preserves its localized nature, and it is separated by an energy gap (threshold) from the delocalized states (magnons). In Fig. 13 we show how breather stability changes as a function of the detuning parameter $\Delta\omega=\omega_b-\Omega_\pi$. In panel (a) we show how the breather energy E (normalized to the energy of the ferromagnetic ground state) depends on the detuning. The energy threshold is clearly seen as it is the minimum of the function $E(\Delta\omega)$. Panels (b) and (c) show the development of the Floquet eigenvalues. It can be clearly seen that the breather becomes unstable long before the magnon upper edge is reached. The instability is caused by parametric resonances of magnons first, and by parametric resonance of the internal mode later. Additional bifurcation occurs when E attains its minimum.

V. TWO-DIMENSIONAL LATTICE WITH EASY-PLANE ANISOTROPY

Finally, we briefly review results[18] on a two-dimensional easy-plane ferromagnet with nearest-neighbor exchange interactions. Numerical simulations of the discrete Landau–Lifshitz equations (3) with $\mathbf{n}=\{n,m\}$ using the fourth-order Runge–Kutta scheme with various initial spin configurations have been carried out. The results to some extent are similar to the one-dimensional problem. In Fig. 14 the simplest possible configurations of the breathers that involve four ''out-of-plane'' precessing spins are shown. No stable breathers with one precessing spin are possible, similar to the one-dimensional model. Also, there are no stable breathers with two or three precessing spins (at least, in the limit of small J). Among the three possible stable configurations shown in Fig. 14, the first one [see panel (a)] corresponds to four spins precessing being parallel to each other and in-phase, similar to its one-dimensional counterpart. The second two configurations do not have direct analogs in the one-dimensional case, but they can be considered as a two-dimensional combination of the $(\uparrow\downarrow)$ solution with the $(\uparrow\downarrow)$ (b) or $(\uparrow\uparrow)$ (c) solution. The cases shown in Figs. 14(b) and 14(c) represent the breathers with two spins precessing around the Z-axis in

the positive direction (marked by dots) and two spins precessing around the negative direction (marked by crosses). The simulations have been performed on a lattice of 150 $\times 150$ spins with $J=0.11$ and $D=-1$.

VI. SUMMARY AND DISCUSSIONS

We have presented a review of the previous results and some new results on the discrete breathers in the easy-plane ferromagnetic lattices. We have focused on the essentially discrete solutions which have no continuum analogs. This is due to the fact that the spins in the center of the excitation precess around a tilted axis leading to a local tilt of the magnetization. As a result, this class of discrete breathers possesses energy thresholds (gaps). Note that for lattices of interacting scalar degrees of freedom, the discrete breathers have typically zero lower energy bounds in spatial dimension $d=1$ and become nonzero[22] only for $d=2,3$. The energy of the thresholds depends on the number of precessing ''out-of-plane'' spins. This class of discrete breathers is analogous to rotobreathers which exist in arrays of Josephson junctions.[5] Such energy thresholds may be very important as they show up in contributions to thermodynamic quantities that depend exponentially on temperature. The system supports a rich variety of breather solutions, depending on the number of the precessing spins and their respective orientation. These solutions have been classified and categorized according to their internal structure, and their linear stability have been studied. We find some general rules on how to create stable breathers with the desired structure. In particular, arbitrary sequences of pairs of parallel spins $[(\uparrow\uparrow)$ and $(\downarrow\downarrow)]$ can be created. If such solutions are to be observed experimentally, they can be used to store information.

ACKNOWLEDGMENTS

This work has been supported by LOCNET Project No. HPRN-CT-1999-00163, and by the INTAS Foundation under Grant No. INTAS 97-0368. J.M.K. wishes to acknowledge the support of the Danish Research Agency.

[1] H. Segur and M. D. Kruskal, Phys. Rev. Lett. **58**, 747 (1987).
[2] S. Flach and C. R. Willis, Phys. Rep. **295**, 182 (1998).
[3] S. Aubry, Physica D **103**, 201 (1997).
[4] R. S. MacKay and S. Aubry, Nonlinearity **7**, 1623 (1994).
[5] E. Trias, J. J. Mazo, and T. P. Orlando, Phys. Rev. Lett. **84**, 741 (2000); P. Binder, D. Abraimov, A. V. Ustinov, S. Flach, and Y. Zolotaryuk, *ibid.* **84**, 745 (2000).
[6] H. S. Eisenberg, Y. Silberberg, R. Morandotti, A. R. Boyd, and J. S. Aitchison, Phys. Rev. Lett. **81**, 3383 (1998); R. Morandotti, U. Peschel, H. S. Eisenberg, and Y. Silberberg, *ibid.* **83**, 2726 (1999).
[7] I. Swanson, J. A. Brozik, S. P. Love, G. F. Strouse, A. P. Shreve, A. R. Bishop, W.-Z. Wang, and M. I. Salkola, Phys. Rev. Lett. **82**, 3288 (1999).
[8] A. Xie, L. van der Meer, W. Hoff, and R. H. Austin, Phys. Rev. Lett. **84**, 5435 (2000).
[9] J. Edler, P. Hamm, and A. C. Scott, Phys. Rev. Lett. **88**, 067403 (2002).
[10] For reviews, see V. G. Makhankov and V. K. Fedyanin, Phys. Rep. **104**, 1 (1984); A. M. Kosevich, B. A. Ivanov, and A. S. Kovalev, *ibid.* **194**, 117 (1990); H.-J. Mikeska and M. Steiner, Adv. Phys. **40**, 191 (1991).
[11] A. A. Anders, G. V. Borisenko, and S. V. Volotskii, Fiz. Nizk. Temp. **15**, 39 (1989) [Sov. J. Low Temp. Phys. **15**, 21 (1989)].
[12] M. I. Kobets, A. A. Stepanov, and A. I. Zvyagin, Fiz. Nizk. Temp. **7**, 1473 (1981) [Sov. J. Low Temp. Phys. **7**, 716 (1981)].
[13] S. Takeno and K. Kawasaki, Phys. Soc. Jpn. **60**, 1881 (1991); Phys. Rev. B **45**, 5083 (1992).
[14] R. F. Wallis, D. L. Mills, and A. D. Boardman, Phys. Rev. B **52**, R3828 (1995).
[15] R. Lai and A. J. Sievers, Phys. Rep. **314**, 147 (1999).
[16] M. V. Gvozdikova and A. S. Kovalev, Fiz. Nizk. Temp. **24**, 1077 (1998) [Low Temp. Phys. **24**, 808 (1998)]; Fiz. Nizk. Temp. **25**, 1295 (1999) [Low Temp. Phys. **25**, 972 (1999)].
[17] U. T. Schwarz, L. Q. English, and A. J. Sievers, Phys. Rev. Lett. **83**, 223 (1999).
[18] Y. Zolotaryuk, S. Flach, and V. Fleurov, Phys. Rev. B **63**, 214422 (2001).
[19] M. Speight and P. M. Sutcliffe, J. Phys. A **34**, 10839 (2001).
[20] For simplicity we will denote breathers only using their core part, i.e., $(\cdots 000\uparrow 000\cdots)\equiv(\uparrow)$.
[21] J. L. Marín, S. Aubry, and L. M. Floría, Physica D **113**, 283 (1998).
[22] S. Flach, K. Kladko, and R. S. MacKay, Phys. Rev. Lett. **78**, 1207 (1997).